Design and Simulation of ٢٤GHz TX FMCW RADAR System- Based Drone Detection

Saja Azeez Shalal[١,*] , Moretadha J. Kadhom[٢]

[١,٢]Electrical Department, Engineering College, Baghdad University, Baghdad, Iraq

a) Author email: Saja.aziz٢٣٠٢m@coeng.uobaghdad.edu.iq

b) Email: Moretadha@coeng.uobaghdad.edu.iq

ABSTRACT

This paper presents the design and simulation of a ٢٤ GHz Frequency Modulated Continuous Wave Transmitter radar (TX FMCW) system with a ٢x١ microstrip array antenna specifically for use in aimed at drone detection. Modern radar technology is required for efficient surveillance and monitoring due to the growing use of drones in many industries. To obtain a small and light form factor that may be incorporated into drone detection systems, the suggested antenna design makes use of microstrip technology. The effectiveness of the design is validated through CST Studio and Altium Designer simulation programs. Simulation results demonstrate that the antenna provides high gain (١٠,٣٧ dBi) and sharp beam (٢٣٦ degrees), a favorable radiation pattern, ensuring enhanced detection capabilities over extended ranges. A ٢٥٠MHz bandwidth was sufficient to accommodate the operational requirements of FMCW radar, providing reliable signal transmission. The design is validated by simulation results, including interference simulations, which show that the radar can meet the requirements for operational efficiency in real-world situations. Combining the improved antenna design and TX FMCW Radar with the receiver and signal processing algorithms is an essential next step in putting a complete drone detection system into place.

Keywords: Array, Drone detection, FMCW Radar, Interference, Patch antennas.

المستخلص:

تقدم هذه الورقة تصميما ومحاكاة لنظام رادار إرسال موجة مستمرة معدل بالتردد (TX FMCW) بتردد ٢٤ جيجا هرتز، مزود بهوائي مصفوفة ميكرو ستريب ٢×١، مخصص للاستخدام في رصد الطائرات بدون طيار. وتعد تقنيات الرادار الحديثة ضرورية للمراقبة والرصد بكفاءة نظرا للاستخدام المتزايد للطائرات بدون طيار في العديد من الصناعات. وللحصول على شكل صغير وخفيف الوزن يمكن دمجه في أنظمة رصد الطائرات بدون طيار، يعتمد تصميم الهوائي المقترح على تقنية الميكرو ستريب. وقد تم التحقق من فعالية التصميم من خلال برنامجي محاكاة CST Studio و .Altium Designer وتظهر نتائج المحاكاة أن الهوائي يوفر كسبا عاليا (١٠,٣٧ ديسيبل) وشعاعا حادا (٢٣٦ درجة)، ونمط إشعاع ملائم، مما يضمن قدرات كشف محسنة على نطاقات ممتدة. ويكفي عرض نطاق ترددي يبلغ ٢٥٠ ميجاهرتز لتلبية المتطلبات التشغيلية لرادارFMCW ، مما يضمن نقل إشارة موثوقا. وقد تم التحقق من صحة التصميم من خلال نتائج المحاكاة، بما في ذلك محاكاة التداخل، والتي تظهر أن الرادار قادر على تلبية متطلبات الكفاءة التشغيلية في الظروف الواقعية. إن الجمع بين تصميم الهوائي المحسن ورادار TX FMCW مع خوارزميات الاستقبال ومعالجة الإشارة هو الخطوة التالية الأساسية في وضع نظام كامل لكشف الطائرات بدون طيار.

١. INTRODUCTION

Tracking and identifying drones is crucial for airspace administration and security as their usage for various objectives increases. An excellent replacement for conventional radar programs is frequency-modulated constant wave (FMCW) radar, which can determine the drone's length, velocity, and motion by continuously transmitting a frequency-modulated signal and assessing the returned signal. Detecting slow-moving drones is one of its numerous advantages, along with its fantastic exactness and reduced battery usage. Air traffic monitoring, security, and the military all make extensive use of this technology to identify unapproved drones and stop possible threats. To provide safety and security in a variety of applications, FMCW radar will become increasingly important as drone usage increases. One essential element that directly affects how well the FMCW radar system detects and tracks drones is the transmitter. This study focuses on creating a ٢٤ GHz transmitter FMCW radar for drone detection. Through the creation, amplification, and emission of a modulated signal, it allows the radar to retrieve accurate velocity and range data. ٢ by ١ microstrip patch array antennas are used in the system because of their high gain, low profile, ease of manufacture, ability to steer beams, and appropriateness for high-frequency operation (Mailloux

٢٠١٧) and (Balanis ٢٠١٦). This study was carried out after a comprehensive review of the literature on FMCW radar using microstrip patch array antenna design, which included studies. In ref. (Oh, Guo, and Lin ٢٠١٩), Based on FMCW surveillance radar echo signals, a successful and effective UAV classification system was proposed. The system's five main components were burst selection, rule-based scan pruning, feature extraction from IMFs obtained using the EMD technique, TER-based classification, and scan-to-scan filtering. It was shown that the features recovered from IMFs had discriminative information based on experiments using FMCW radar returns that were physically measured from fixed-wing UAVs, rotary-wing UAVs, and non-UAV objects.

The creation of an algorithm for calculating target distances and speeds in a multi-target scenario using FMCW automobile radar was highlighted in (Kuptsov et al. ٢٠١٩). Through experimental evaluations, it also offers insights into the algorithm's performance and tackles the problems related to incorrect targets. Ref. (Miura et al. ٢٠١٩) used a single compact microcontroller board and a replica radar chipset to present a low-cost distance-spoofing attack on a mm Wave FMCW radar. The attack setup developed in this work is notable for its affordability and lightweight design, as it eliminates the need for expensive and bulky test instruments. Ref. (Pratiwi et al. ٢٠١٩) suggested enhancements to the FMCW radar system to identify minute respiratory activity-related displacements in the belly or chest wall. The conventional FMCW radar concept requires a large bandwidth for this purpose. The paper presents the concept of phase detection as a means to enhance the capability of FMCW radar in detecting small displacements. Ref. (Musa et al. ٢٠١٩) conducted a comprehensive review of the current state of the art in drone detection methods, with a focus on radar systems that utilize micro-Doppler-based analysis. Additionally, they introduce the concept of passive forward scatter radar (PFSR) as a promising emerging methodology for both ground and airborne target detection. By leveraging digital video broadcasting satellite (DVBS) technology, it highlights its enhanced capabilities. This proposed

method aims to make micro-Doppler analysis for low-profile targets, specifically, copter drones, a feasible and effective endeavor. Ref. (Park et al. ٢٠٢١) proposed a solution to the persistent problem in FMCW radar systems, which is the leakage from the transmitter to the receiver. This paper proposes a technique called the stationary point concentration technique to mitigate this problem. The proposed technique does not require additional hardware and can be implemented through frequency planning and digital signal processing. The results of the study demonstrate that the proposed technique significantly reduces the noise floor within the desired range domain. Ref (Coluccia, Parisi, and Fascista ٢٠٢٠) focused on the problem of drone identification, detecting, verifying, and classifying drones. It provides an overview of the relevant technologies used in contemporary surveillance systems, which typically consist of a network of spatially distributed sensors to ensure comprehensive coverage of the monitored area. One technology highlighted in the paper is the FMCW radar sensor. Ref (Zulkifli and Balleri ٢٠٢٠) discussed the design and development of a prototype K-Band FMCW radar system for the detection of nano drones. The FMCW radar prototype utilizes connectorized components operating at a carrier frequency of ٢٤ GHz, providing a high degree of flexibility in parameter selection. The results demonstrate that the radar system is capable of detecting a small-sized Arcade PICO Drone Nano Quadcopter, which is smaller than ٥ cm. Furthermore, the micro-Doppler signature of the detected nanodrone could be extracted from the collected data. In ref. (Han and Hong ٢٠٢١), a multiple-input and multiple-output (MIMO) FMCW radar system is suggested as a means of detecting individuals in several locations. Digital beamforming using virtual receiver arrays acquired by time-division multiplexing (TDM) MIMO radar operation is used to estimate a ٢-D range-angle map. By utilizing the standard deviation of phase variations, the suggested approach can get beyond a conventional method's codomain constraint. The project (Salih et al. ٢٠٢٥) concentrated on developing a transportable single-axis solar tracker that used satellite dish actuators to precisely track the sun's path and

astronomical mathematics and GPS technology to identify the sun's position in the sky precisely.

The primary objective of this study is to design a transmitter FMCW radar-based drone detection system and a ٢ x ١ microstrip patch array antenna with different phase shifts. The design focuses on high directivity for improved detection range and sensitivity, wide bandwidth to detect drones of various sizes and speeds, low sidelobe levels to minimize interference, and efficient beam steering for precise tracking. CST Microwave Studio and Altium Designer will be used for electromagnetic simulations to model and optimize the radar. The results will be validated based on directivity, main lobe magnitude, main lobe direction, angular width, and sidelobe levels to ensure the design meets performance requirements.

٢. METHODOLOGY

٢.١. Radar Equation

A radar operating system's basic premise is that a radar transmitter emits radio waves, which travel through space and collide with an object before being reflected and returned to the radar receiver. Radar systems utilize the properties of the reflected signal to determine the target's velocity, range, and, in some more sophisticated systems, its form. Target, environment, transmitter, receiver, and antenna all affect the power of the received signal. The radar equation considers these factors while calculating the received signal power. This equation is also used to assess trade-offs while developing a radar system (Rameez ٢٠٢٠). The radar equation's fundamental form is:

$$P_r = \frac{P_t\, G_t G_r \sigma \lambda^2}{(4\pi)^3 R^4 L \alpha} \quad (1)$$

where $P_t, G_t, G_r, \sigma, \lambda, R, L,$ and α are the transmitted power, the transmitting antenna's gain, the receiving antenna's gain, the target's radar cross-section, the

wavelength of the transmitted signal, the distance between the radar and the target, the system loss factor, and the medium attenuation factor, respectively. For a monostatic radar configuration, $G_t = G_r$.

The distance at which the radar detects the least amount of backscattered power P_{min} is known as the maximum radar range R_{max}, and it can be computed as follows:

$$R_{max} = \left(\frac{P_t G^2 \lambda^2 \sigma}{(4\pi)^3 L \alpha P_{min}}\right)^{1/4} \quad (2)$$

In the equation above, the radar system and propagation medium are considered to be lossless. However, the method does not account for various other factors that could affect it, such as noise, loss, weather conditions, and other considerations.

٢,٢. FMCW RADAR model

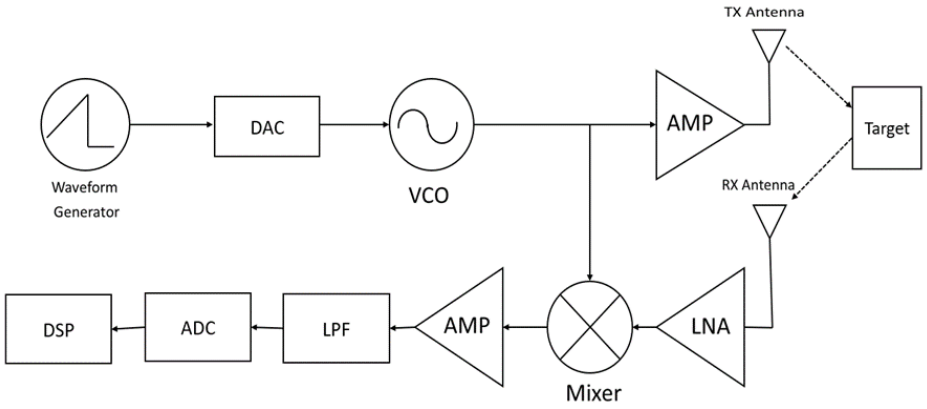

Figure ١. Block diagram of the FMCW Radar system(Resolution ٢٠٢١)

Fig. ١ shows a block diagram of a ٢٤ GHz FMCW Radar system, which consists of a waveform generator that generates a linear transmission waveform, a digital-to-analog converter (DAC), a voltage control oscillator (VCO) that modulates the frequency of the transmission signal, and an amplifier. The signal is then transmitted through the transmitter antenna TX to the target.

The transmitted signal is a continuous waveform whose frequency changes linearly (increases or decreases) over time (called chirp), see **Fig. ٢**, which is defined by equation (٣)(Heo et al. ٢٠٢١).

$$F(t) = fc + \alpha t \qquad (٣)$$

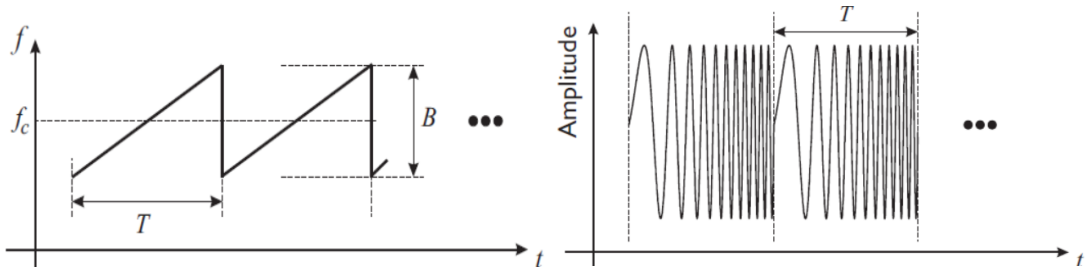

Figure ٢. FMCW radar's transmitted waveform (a) Instantaneous frequency (b) Amplitude as a function of time

where T is the period, B is the bandwidth, t is the duration, fc is the carrier frequency, and α is the chirp rate, which is equal to B/T.

The transmission waveform's frequency can be integrated for time to determine the waveform's instantaneous phase φ, as in equation (٤).

$$\varphi(t)=٢\pi\int_{٠}^{t} f(t)dt=٢\pi\int_{٠}^{t}(f_c + \alpha t)dt=٢\pi\,(f_c\,t+\frac{\alpha t^{٢}}{٢}) \qquad (٤)$$

The time-domain description of the first chirp of the transmission signal is given by Equation (٥), where A is the signal's amplitude.

$$S_{TX}(t)=A\cos(\varphi(t)) = A\cos\,(٢\pi\,(f_c\,t+\frac{\alpha t^{٢}}{٢})) \qquad (٥)$$

A target echo signal is produced when the transmitted waveform reaches the receiving antenna, RX, after a propagation delay, and is reflected off of objects in the field of view. $S_{RX}(t)$, as shown in Fig. ٣. (Resolution ٢٠٢١)

$$S_{RX}(t)= A\cos(٢\pi(f_c(t-\tau) +\frac{\alpha(t-\tau)^{٢}}{٢})) \qquad (٦)$$

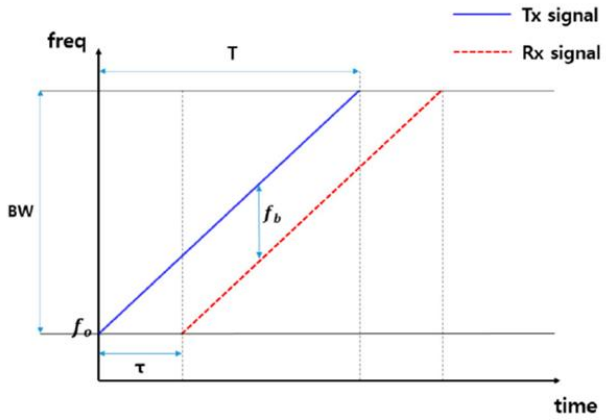

Figure ٣. The transmission and reception signals of FMCW radar sawtooth waves

To get a signal with the same frequency as the transmitted signal, the echo signal was passed through a low-noise amplifier (LNA). The returned signal and the transmitted signal are mixed by multiplying the two signals together. After mixing, the high-frequency signal is removed by a low-pass filter (LPF), leaving only the low-frequency signal, which is referred to as the beat frequency.

$$S_{beat}(t)=\frac{A^{٢}}{٢}\cos\left(٢\pi f_b t+\varphi\right) \qquad (٧)$$

An analog-to-digital converter (ADC) is used to transform an analog signal into a digital signal. FFT (Fast Fourier Transform) is used in the DSP (digital signal processing) stage to derive the beat frequency from the digital stream, and then the range R and velocity V of the target by the following equations:

$$R=\frac{Cf_b}{٢\alpha} \qquad (٨)$$

$$V=\frac{f_d\lambda}{٢} \qquad (٩)$$

٢،٣. FMCW design

Utilizing connectorized monolithic microwave integrated circuit (MMIC) components from Analog Devices, working in the ٢٤ GHz ISM band. The radar system electronics included a ٢-channel transmitter chip (ADF٥٩٠١), a ٤-channel receiver chip (ADF٥٩٠٤), and a phase-lock loop (PLL) and voltage-controlled

oscillator (VCO) (ADF٤١٥٩). It operates at a maximum frequency of ١٣ GHz. The ADAR٧٢٥١, a ٤-channel continuous-time analog-to-digital converter (ADC) with ١٦-bit resolution, was used to sample the data before sending it to the digital signal processor (DSP) (see Fig. ٤).

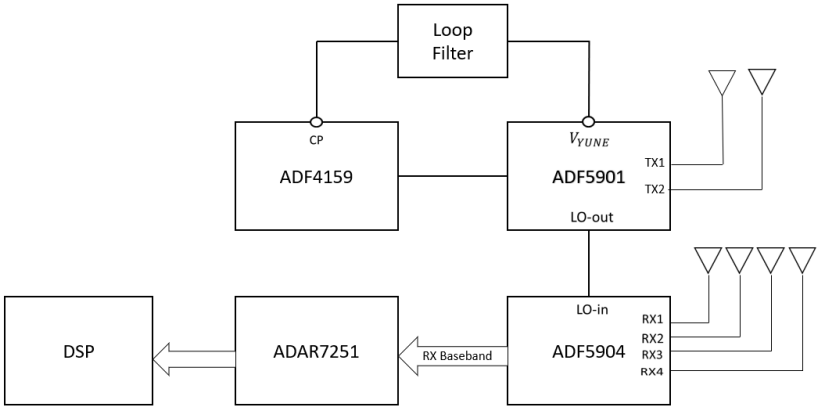

Figure ٤. Schematic of FMCW Radar design

٢,٤. Transmitter software design

A transmit stage is necessary to interface with an antenna and effectively propagate the sent radar signal by providing the FMCW ramp with sufficient gain. As mentioned in the radar equation, the range of the radar depends on the strength of the transmitted signal. The MMIC transmit IC ADF٥٩٠١ (Downconverter, n.d.) is an incorporated option. It contains an integrated divide-by-٢ output and a ٢٤ GHz to ٢٤,٢٥ GHz VCO. Additionally, the ADF٥٩٠١ features a ٢-channel ٢٤ GHz power amplifier (PA) at its output, capable of providing power up to ٨ dBm, as well as a local oscillator (LO) output buffer. See **Fig. ٥**.

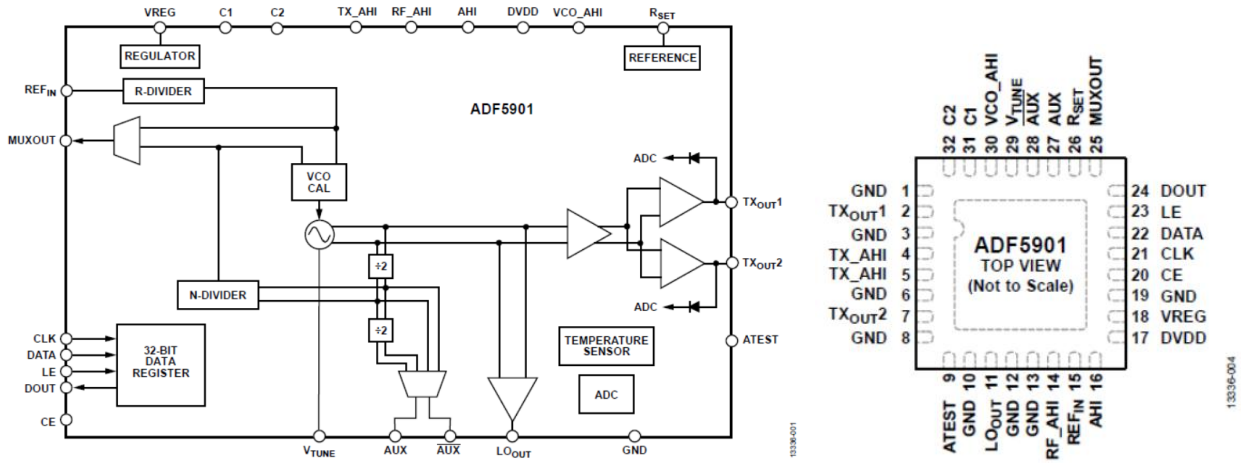

Figure ٥. ADF٥٩٠١ (a)functional block diagram, (b)bin configuration.(Sheet ٢٠١٧)

To design the transmitter, Altium Designer is used for creating PCB electronic circuit boards. **Fig.** ٦ shows the schematic design, which contains the ADF٥٩٠١WCCPZ, a ٢٤ GHz FMCW radar transmitter chip, a low-pass filter, a test pin, a load enables LE, and a switch IC for power distribution. This component provides controlled starting, thermal shutdown, and overcurrent protection, in addition to managing power distribution from a source to a load. The chip enables the CE pin's logic low, shutting off the device. Considering the state of the power-down bit, turning the pin high activates the gadget. The part number, manufacturer, and power supply of these components are shown in Table ١, and the resistor and inductor values are shown in **Table** ٢.

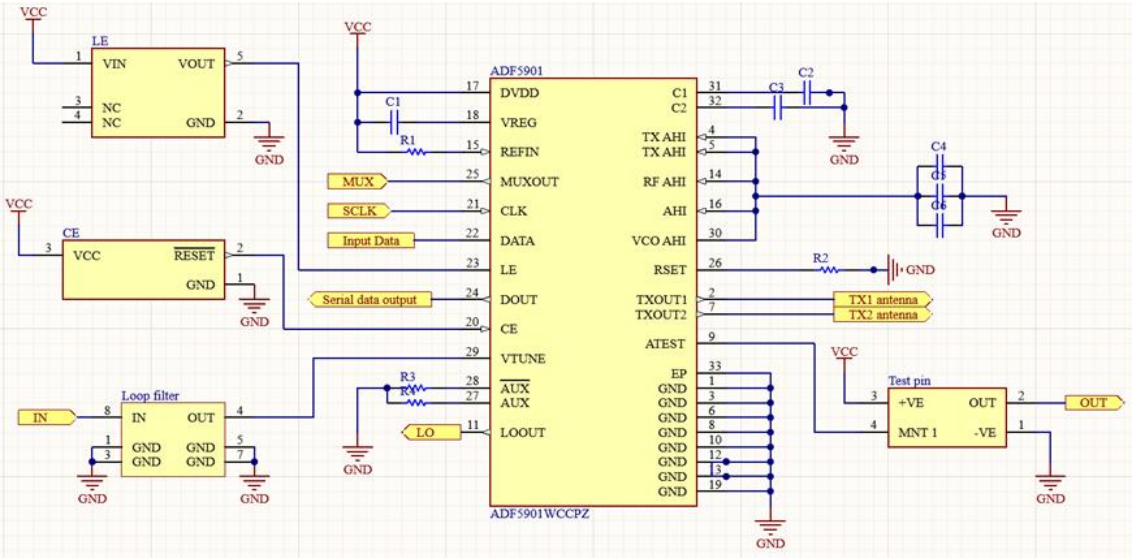

Figure ٦. Schematic design in Altium designer.

Table ١. The part number, manufacturer, and power supply of the FMCW radar transmitter. Components

Transmitter part	Part number	Manufacturer	Power supply(V)
ADF٥٩٠١	ADF٥٩٠١WCCPZ	Analog Devices	٣,٣
LE	MIC٢٠٠٣-٠,٥YM٥-TR	Microchip Technology	٢,٥-٥,٥
CE	ADM٨٠٩JARTZ-REEL٧	Analog Devices	١,٠-٥,٥
Loop Filter	٧٤٨١١١٠٠٩	Wurth Electronics	-
Test pin	HIH-٥٠٣١-٠٠١	Honeywell Sensing and Productivity Solutions	٢,٧-٥,٥

Table ٢. Resistors and inductors of the FMCW radar transmitter values

Component	Value	Component	Value
C١	٠,٢٢μF	**C٦**	١٠pF
C٢	٤٧nF	**R١**	١٠٠KΩ
C٣	٠,٢٢μF	**R٢**	٥,١KΩ
C٤	٠,١μF	**R٣**	٥٠Ω
C٥	١nF	**R٤**	٥٠Ω

Fig. ٧ shows the arrangement of components on a two-layer printed circuit in ٢D and ٣D layout modes. The printed circuit board is designed according to specific rules and restrictions; for example, the minimum clearance is ٠,٠٣ mm, routing corners are ٤٥ degrees with a setback ٢,٥٤ mm, the via diameter is ١,٢٧ mm, the

routing track's width ranges from ٠,٠٤ mm to ٠,١٨ mm, and the permissible routing layers are the top and bottom layers.

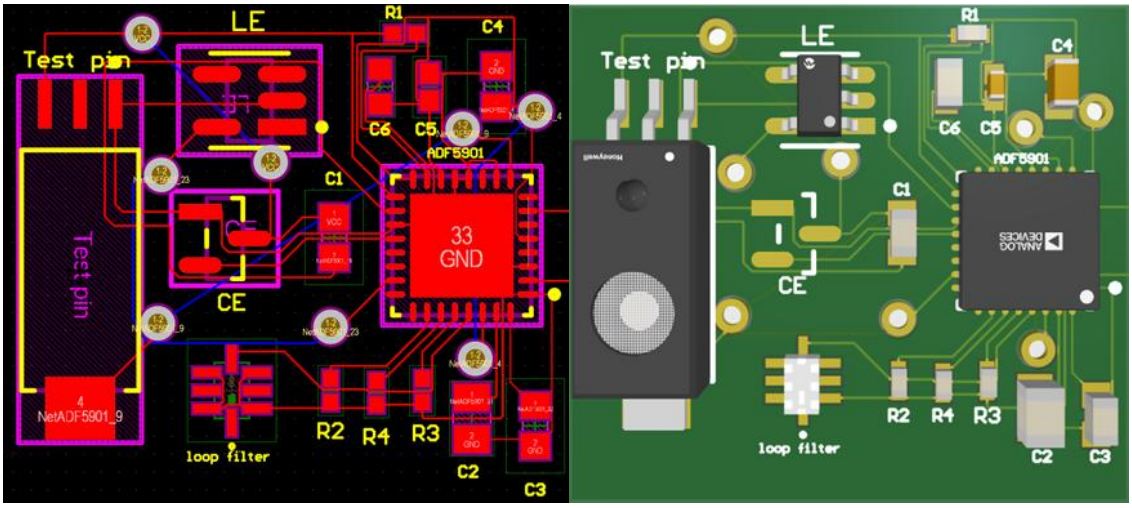

(a) **(b)**

Figure ٧. The printed circuit board is designed by an Altium designer in (a)٢D (b)٣D layout mode.

To simulate the printed circuit board and connect it to the antenna, the CST Studio program was used by exporting the board to an ODB++ file and then importing it into CST; see **Fig. ٨a**. After that, the third layer (base) was constructed using a PEC material with a thickness of ٠,٠٤ mm, and the components were imported via a step file from their manufacturer. The dimensions of the designed board are ٢٠,٩٦ mm x ١٨,٥٤ mm, and two microstrip patch antenna arrays are connected to the board, whose dimensions are ٢,٦٨ mm x ٥,٣٧ mm for the substrate (٠,٠٧ mm height) and the PEC patch (٠,٠١ mm height). The PEC patch dimensions are ١,١٨ mm x ١,٤١ mm with a height of ٠,٠١ mm, as shown in Fig. ٨ b.

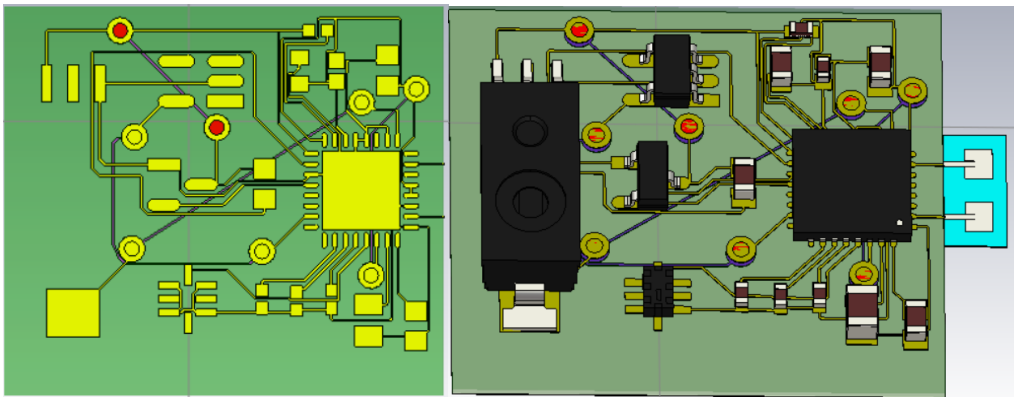

(a) (b)

Figure ٨. The printed circuit board by CST studio on (a)two layers, (b)three layers with antenna

٣. SIMULATION RESULTS AND DISCUSSION

٣،١. S-Parameter

The S-parameter plot of the input data port on the designed board (pin ٢٢ in the schematic design in Fig. ٦) is presented in Fig. ٩. At ٢٤،٠٥٦ GHz, the reflection is lowest (−١،٢٦٧ dB), indicating that at this frequency, the port is best matched. Most of the power is transmitted rather than reflected. The lower the S-parameter value, the better the impedance matching at that frequency, and the port's performance is best (Prabowo, Pambudiyatno, and Harianto ٢٠٢١).

Fig. ١٠ shows the S-parameter plot of the output data (pin ٢٤ in the schematic design in Fig. ٦). The best performance of the port occurs at a frequency of ٢٤،٠٢٤ MHz, where the reflection is lowest (-٢،٤٢١ dB).

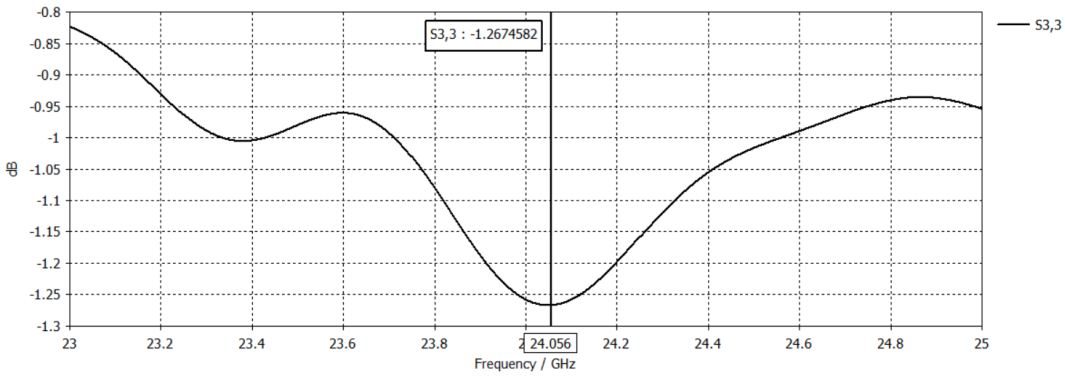

Figure ٩. S Parameter plot of the input port of the designed board.

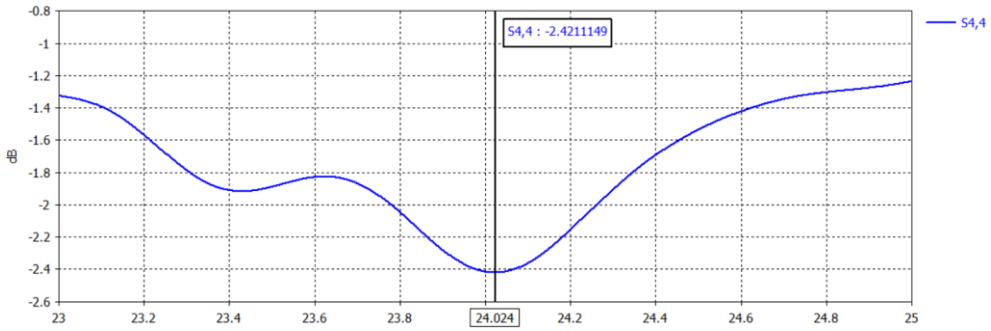

Figure ١٠. S Parameter plot of an output port of the designed board.

٣،٢. Far-field of the antenna

The far-field calculation of antenna arrays' phase shift is a key concept in understanding how arrays create beams and direct them in desired directions. **Fig.** ١١ shows the ٣D far-field directivity plot for four phase shift angles (٠°, -٩٠ °, -١٨٠ °, and -٢٧٠ °), while Fig. ١٢ shows the polar plot of the radiation pattern (φ in degrees) for these angles. From these simulation plots, we can compute the directivity, main lobe magnitude, main lobe direction, angular width, and side lobe level; see **Table ٣**.

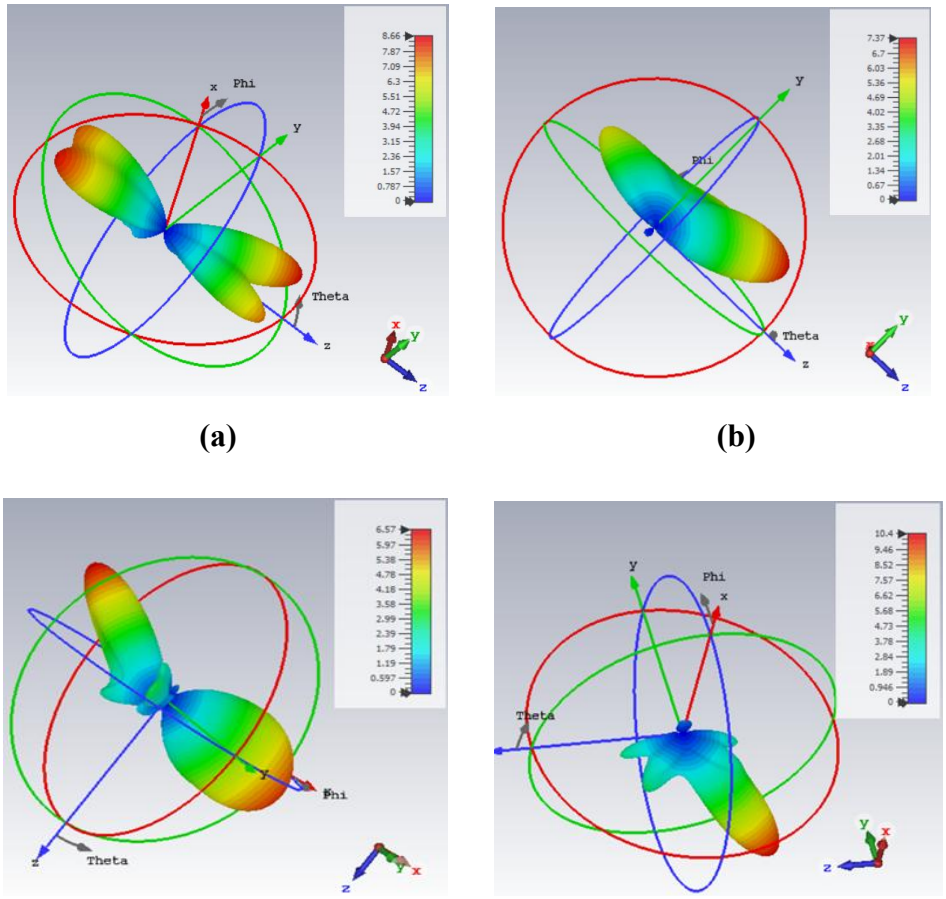

(a) (b)

(c) (d)

Figure ١١. ٣D Far-field directivity plot for (a) ٠ (b)-٩٠°(c)-١٨٠°(d)٢٧٠° phase shift of antenna array.

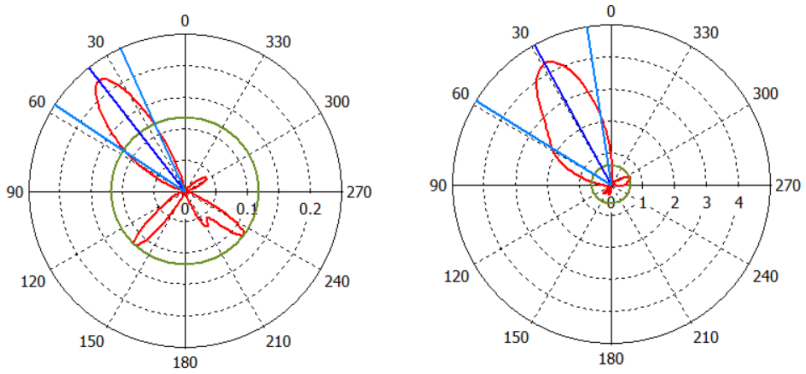

(a) (b)

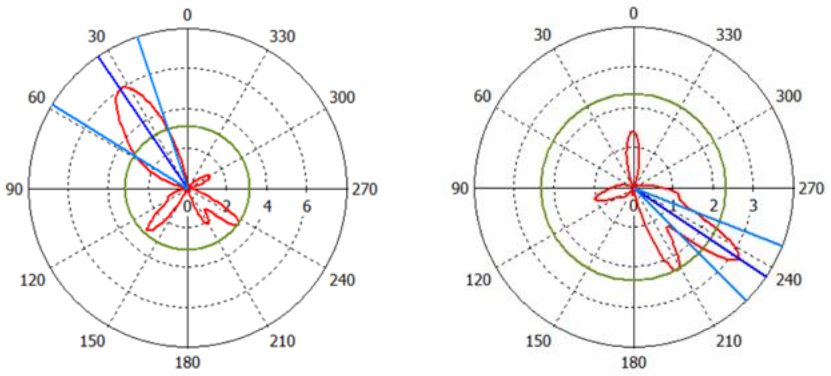

(c) (d)

Figure ١٢. Polar plot of the radiation pattern (phi in degrees) at (a)٠, (b)-٩٠°, (c)-١٨٠°, (d)-٢٧٠° phase shift of antenna array.

Table ٣.The most important results from a simulation of ٣D Far-field directivity and Polar plot

Phase shift	Directivity (dBi)	Main lobe magnitude (w/m٢)	Main lobe direction (degree)	Angular width (degree)	Side lobe level(dB)
٠	٨,٦٦٠	٠,٢٢٣	٣٨,٠	٣٢,٢	-٢,٧
-٩٠°	٧,٣٧٢	٤,٣٣	٢٩,٠	٤٩,٦	-٨,٣
-١٨٠°	٦,٥٧٢	٦,٠١	٣٤,٠	٤٠,١	-٢,٨
-٢٧٠°	١٠,٤١	٣,١٦	٢٣٦,٠	٢٣,٦	-١,٣

The results in **Table** ٣ show that the -٢٧٠ ° phase shift yields the highest directivity (١٠,٤١ dBi) and sharpest beam (٢٣٦ degrees), as well as the highest radiation efficiency (٩٩,٢٨٤٪), but exhibits very poor side lobe suppression (−١,٣ dB), which risks more false detections. In contrast, a −٩٠° phase shift provides the best side lobe suppression (−٨,٣ dB), albeit with a wider beam at ٤٩ degrees (resulting in less targeting precision) and lower directivity (٧,٣٧٢ dBi). The most essential features of radar applications in drone detection are directivity, range, and accuracy; therefore, the -٢٧٠ ° phase shift is the best choice for these applications.

٣,٣. Interference

To understand how undesired signals (interference) affect system design, such as unwanted coupling between ports and mutual interference in arrays, a schematic

was created, and the ports whose interference behavior was to be understood were identified—Fig. ١٣a. The violation matrix(shown in **Fig. ١٣ b) shows for all Rx (Receiver Import Band),** Tx (Transmitter Import Band) combinations if there are violation events. The red squares with a cross represent margins above ٠ dB that are always considered as violation events. Margins above the user-defined threshold are shown as yellow squares with an exclamation mark. If no violation event occurs for an Rx-Tx combination, there is a green square with a check. For uncoupled receivers and transmitters, there is no square shown at all. Rx١ (receiver of first antenna TX١) works safely with clock port CLK, Tx١, and Tx٢. Not allowed with the transmitter of the input data port; this does not affect when connecting an integrated circuit of the radar. Rx٢ (receiver of the second antenna) works safely with Clk, Tx٢, and Tx٣. Caution with Tx١ (yellow): possible minor interference or special requirements. InRx٣ (receiver of input data port) works safely with Clk, Tx٢, and Tx٣. Not allowed with Tx١; this does not affect when connecting an integrated circuit of the radar.

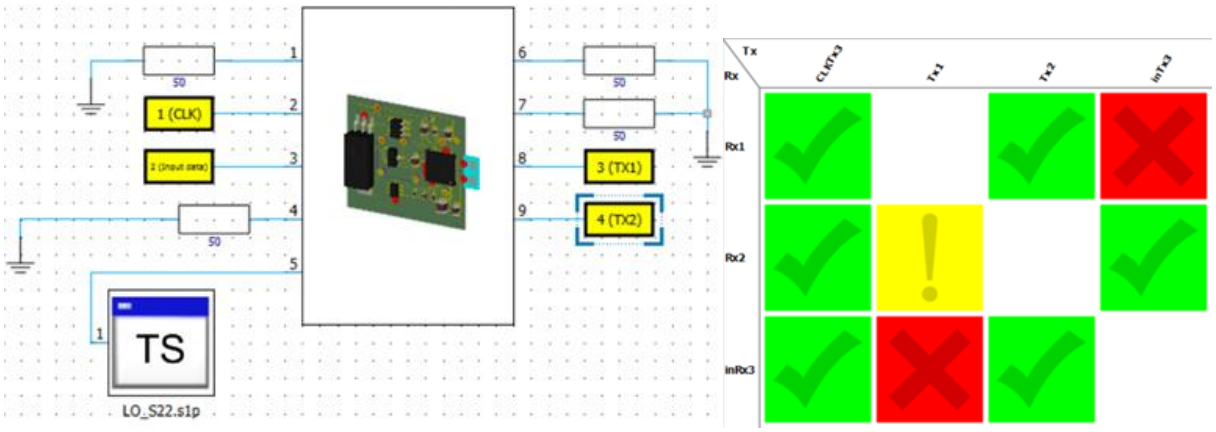

Figure ١٣. TX FMCW Radar in CST Studio: (a) schematic, (b) main violation matrix showing Rx-Tx combinations

Our study was compared with previous works on the same type of radar (FMCW). It was found that, at a frequency of ٢٤ GHz, our design, despite its small size (٢٠,٩

mm x ١٨,٥٤ mm) and simple antenna, yielded a gain value of ١٠,٣٧ dBi, which is relatively high. A ٠,٢٥ GHz bandwidth for a TX FMCW radar means the system can transmit signals over a wide frequency range, improving its ability to detect and analyze the presence and behavior of drones effectively. By applying the radar range equation (٢) and taking into account the simulation results, the value of the distance was obtained as ١٧,٥ m, which is an appropriate value for short-range radar applications. The range can be increased by improving the antenna or increasing the output power through a power amplifier.

Table ٤. Comparison of this study with the earlier studies.

Ref. year	Dimension (mm)	Frequency (GHz)	Antenna Type	Gain (dBi)	BW (GHz)	Rang (m)
[This Ref.]	٢٠,٩x ١٨,٥٤	٢٤	٢by١ microstrip patch array	١٠,٣٧	٠,٢٥	١٧,٥
(Will et al. ٢٠١٩)	٤٥x٥٠	٢٤	series-fed ١x٦ linear array	٢٣,٥	٠,٢	٢٠
(Hansen et al. ٢٠٢٠)	١٠x٥	٦١/١٢٢	differential fed patch	٧,٥	٨	٢٣,٣
(Ash, Ritchie, and Chetty ٢٠١٨)	-	٥,٨	Yagi	١٢	٠,١٥	٥٠
(Jardak et al. ٢٠١٩)	١٠ x ٤	٢٤-٢٤,٢٥	Five elements array	١١,٤	٠,٢٥	٣٧,٥
(El-Awamry et al. ٢٠٢٤)	-	٢,٤/٤,٨	Two dipoles	٧	٠,٢	٣

٤. CONCLUSIONS

This paper investigates the design and simulation of ٢٤ GHz transmitter FMCW radar systems with a ٢ × ١ microstrip patch array antenna for drone detection targeting. For short-range drone detection applications, the -٢٧٠° phase shift array antenna offers a maximum gain of more than ١٠ dBi, as well as the sharpest beam (٢٣٦ degrees), the highest radiation efficiency, and a bandwidth (٠,٢٥ GHz) sufficient to accommodate the operational requirements of FMCW radar, ensuring reliable signal transmission. Simulation results, including interference simulations, validate the design, indicating that the designed radar can meet the necessary specifications for operational efficiency in real-world scenarios. A crucial next step towards implementing a complete drone detection system will be merging the enhanced antenna design and TX FMCW radar with the receiver and signal processing algorithms.

REFERENCES

١) **Ash, Matthew, Matthew Ritchie, and Kevin Chetty. ٢٠١٨. "On the Application of Digital Moving Target Indication Techniques to Short-Range FMCW Radar Data." *IEEE Sensors Journal* ١٨ (١٠): ٤١٦٧–٧٥.**

٢) **Balanis, Constantine A. ٢٠١٦. *Antenna Theory: Analysis and Design*. John wiley & sons.**

٣) **Coluccia, Angelo, Gianluca Parisi, and Alessio Fascista. ٢٠٢٠. "Detection and Classification of Multirotor Drones in Radar Sensor Networks: A Review." *Sensors* ٢٠ (١٥): ٤١٧٢.**

٤) **Downconverter, MMIC. n.d. "HIGH PERFORMANCE INTEGRATED ٢٤ GHz FMCW RADAR TRANSCEIVER CHIPSET FOR AUTO AND INDUSTRIAL SENSOR APPLICATIONS."**

٥) **El-Awamry, Ahmed, Feng Zheng, Thomas Kaiser, and Maher Khaliel. ٢٠٢٤. "Harmonic FMCW Radar System: Passive Tag Detection and Precise Ranging Estimation." *Sensors* ٢٤ (٨): ٢٥٤١.**

٦) **Han, Kawon, and Songcheol Hong. ٢٠٢١. "Detection and Localization of Multiple Humans Based on Curve Length of I/Q Signal Trajectory Using MIMO FMCW Radar." *IEEE Microwave and Wireless Components Letters* ٣١ (٤): ٤١٣–١٦.**

٧) **Hansen, Steffen, Christian Bredendiek, Gunnar Briese, and Nils Pohl. ٢٠٢٠. "A Compact Harmonic Radar System with Active Tags at ٦١/١٢٢ GHz ISM Band in SiGe BiCMOS for Precise Localization." *IEEE Transactions on Microwave Theory and Techniques* ٦٩ (١): ٩٠٦–١٥.**

٨) **Heo, Jinmoo, Yongchul Jung, Seongjoo Lee, and Yunho Jung. ٢٠٢١. "FPGA Implementation of an Efficient FFT Processor for FMCW Radar Signal Processing." *Sensors* ٢١ (١٩): ٦٤٤٣.**

٩) **Jardak, Seifallah, Mohamed Slim Alouini, Tero Kiuru, Mikko Metso, and Sajid Ahmed. ٢٠١٩. "Compact MmWave FMCW Radar: Implementation and Performance Analysis." *IEEE Aerospace and Electronic Systems Magazine* ٣٤ (٢): ٣٦–٤٤. https://doi.org/١٠,١١٠٩/MAES.٢٠١٩,١٨٠١٣٠.**

١٠) **Kuptsov, Vladimir D, Sergei I Ivanov, Alexander A Fedotov, and Vladimir L Badenko. ٢٠١٩. "Features of Multi-Target Detection Algorithm for Automotive FMCW Radar." In *International Conference on Next Generation Wired/Wireless Networking*, ٣٥٥–٦٤. Springer.**

١١) **Mailloux, Robert J. ٢٠١٧. *Phased Array Antenna Handbook*. Artech house.**

١٢)Miura, Noriyuki, Tatsuya Machida, Kohei Matsuda, Makoto Nagata, Shoei Nashimoto, and Daisuke Suzuki. ٢٠١٩. "A Low-Cost Replica-Based Distance-Spoofing Attack on Mmwave Fmcw Radar." In *Proceedings of the 3rd ACM Workshop on Attacks and Solutions in Hardware Security Workshop*, ٩٥–١٠٠.

١٣)Musa, S Alhaji, RSAR Abdullah, Aduwati Sali, Alyani Ismail, Nur Emileen Abdul Rashid, Idnin Pasya Ibrahim, and Asem Ahmad Salah. ٢٠١٩. "A Review of Copter Drone Detection Using Radar Systems." *Def. S&T Tech. Bull* ١٢ (١): ١٦–٣٨.

١٤)Oh, Beom-Seok, Xin Guo, and Zhiping Lin. ٢٠١٩. "A UAV Classification System Based on FMCW Radar Micro-Doppler Signature Analysis." *Expert Systems with Applications* ١٣٢:٢٣٩–٥٥.

١٥)Park, Junhyeong, Jun-Sung Park, Kyung-Bin Bae, and Seong-Ook Park. ٢٠٢١. "Advanced Stationary Point Concentration Technique for Leakage Mitigation and Small Drone Detection with FMCW Radar." *IEEE Transactions on Microwave Theory and Techniques* ٦٩ (٣): ١٧٩١–١٨٠٤.

١٦)Prabowo, A S, N Pambudiyatno, and B B Harianto. ٢٠٢١. "Microstrip Antenna Design with Patch Rectanguler for Primary Surveillance Radar (PSR) L-Band Application." In *Journal of Physics: Conference Series*, ١٨٤٥:١٢٠٣٣. IOP Publishing.

١٧)Pratiwi, Hana, Mujib R Hidayat, A A Pramudita, and Fiky Y Suratman. ٢٠١٩. "Improved FMCW Radar System for Multi-Target Detection of Human Respiration Vital Sign." *Jurnal Elektronika Dan Telekomunikasi* ١٩ (٢): ٣٨–٤٤.

١٨)Rameez, Muhammad. ٢٠٢٠. "Interference Mitigation Techniques in Fmcw Automotive Radars." Blekinge Tekniska Högskola.

١٩)Resolution, Improving Range. ٢٠٢١. "Improving Range Resolution."

٢٠)Salih, Rizgar Ahmed, Karzan Qadir Mohammed, Peshawa Osman Hama, Rawaz Othman Hassan, and Barham Kamal Noori. ٢٠٢٥. "Design and Implementation of Single Axis Solar Tracking System: Utilizing GPS, Astronomical Equations, and Satellite Dish Actuator for Optimal Efficiency." *Journal of Engineering* ٣١ (٢): ٩٥–١٠٩.

٢١)Sheet, Data. ٢٠١٧. "٢٤ GHz VCO and PGA with ٢-Channel PA Output."

٢٢)Will, Christoph, Prachi Vaishnav, Abhiram Chakraborty, and Avik Santra. ٢٠١٩. "Human Target Detection, Tracking, and Classification Using ٢٤-GHz FMCW Radar." *IEEE Sensors Journal* ١٩ (١٧): ٧٢٨٣–٩٩.

٢٣)Zulkifli, Safiah, and Alessio Balleri. ٢٠٢٠. "Design and Development of K-Band FMCW Radar for Nano-Drone Detection." In *2020 IEEE Radar Conference*

(RadarConf20), ١–٥. IEEE.